

1 **From days to decades: Numerical modeling of freshwater lens response to climate**
2 **change stressors on small low-lying islands**

3 S. Holding^{1,2} and D.M. Allen¹

4 ¹ Department of Earth Sciences, Simon Fraser University, 8888 University Drive,
5 Burnaby, British Columbia, Canada, V5A 1S6.

6 ² Corresponding Author. Email: sholding@sfu.ca

7 Abstract

8 Freshwater lenses on small islands are vulnerable to many climate change related
9 stressors, which can act over relatively long time periods, on the order of decades (e.g.
10 sea level rise, changes in recharge), or short time periods, such as days (storm surge
11 overwash). This study evaluates response of the freshwater lens on a small low-lying
12 island to various stressors. To account for the varying temporal and spatial scales of the
13 stressors, two different density-dependent flow and solute transport codes are used:
14 SEAWAT (saturated) and HydroGeoSphere (unsaturated/saturated). The study site is
15 Andros Island in The Bahamas, which is characteristic of other low-lying carbonate
16 islands in the Caribbean and ~~South~~-Pacific regions. In addition to projected sea level rise
17 and reduced recharge under future climate change, Andros Island experienced a storm
18 surge overwash event during Hurricane Francis in 2004, which contaminated the main
19 wellfield. Simulations of reduced recharge result in a greater up to 19% loss of freshwater
20 lens volume (up to 19%), while sea level rise contributes a lower volume loss (up to 5%)
21 due to the flux-controlled conceptualisation of Andros Island, which limits the impact of
22 sea level rise. volume loss. Reduced recharge and sea level rise were simulated as
23 incremental instantaneous shifts. The lens responds relatively quickly to these stressors,
24 within 0.5 to 3 years, with response time increasing as the magnitude of stressor
25 increases. Simulations of the storm surge overwash indicate that the freshwater lens
26 recovers over time; however, prompt remedial action can restore the lens to potable
27 concentrations up to one month sooner.

28 1. Introduction

29 Small islands are particularly vulnerable to stressors associated with climate
30 change. The freshwater lens is generally sensitive to hydrological disturbances, as a
31 consequence of the low hydraulic gradient and limited thickness of the lens (Vacher,
32 1988; Falkland, 1991; Robins and Lawrence, 2000; White and Falkland, 2010). As
33 groundwater recharge is the primary source of ~~fresh-water~~freshwater to a freshwater lens,
34 an adequate amount of recharge is critical for maintaining the lens morphology (Falkland,
35 1991). Changes in groundwater recharge due to climate change are likely to result from
36 increases in temperature and changes in the spatial distribution, frequency and magnitude
37 of precipitation (Green et al., 2011). Conditions of reduced recharge disturb the balance
38 of freshwater outflow necessary to maintain the extent of the freshwater lens, and may
39 lead to loss of freshwater volume due to saltwater intrusion (Oude Essink, 2001; Ranjan
40 et al., 2009).

41 Sea level rise may result in inundation and a landward shift of the saltwater
42 interface, particularly on low-lying islands (Bear et al., 1999). This would result in a loss
43 of freshwater lens volume, either by a reduction in areal extent and/or a thinning of the
44 lens (Oude Essink, 2001). Projected changes in the frequency of hurricanes and tropical
45 storms are uncertain (Intergovernmental Panel on Climate Change (IPCC), 2014);
46 however, there is evidence to suggest that storms may become more intense, increasing
47 the likelihood of storm surge occurrence (Biasutti et al., 2012). Storm surge overwash can
48 lead to salt contamination of the freshwater lens and a temporary loss of ~~fresh~~
49 ~~water~~freshwater (Anderson, 2002; Illangasekare et al., 2006; Terry and Falkland, 2010).
50 Due to topography, low-lying islands are more susceptible to saltwater inundation from
51 sea level rise and storm surge overwash.

52 Previous modeling studies have investigated aspects of climate change impacts on
53 the freshwater lenses of islands or coastal aquifers. Simulations of decreased recharge
54 resulted in more saltwater intrusion and impact to water supply infrastructure than

55 simulations of sea level rise alone (Rasmussen et al., 2013). However, for regions with
56 future projected increases in recharge, the impact of sea level rise and other stresses (i.e.
57 increases in pumping) may be counteracted by increased recharge (Sulzbacher et al.,
58 2012). Analytical and numerical models of sea level rise indicate that the degree of
59 saltwater intrusion (or loss of freshwater lens volume) resulting from sea level rise
60 depends on many factors. Whether the hydrogeological system is recharge-limited or
61 topography-limited (Michael et al., 2013) influences whether or not the water table rise
62 that accompanies sea level rise can be accommodated by the system. Werner and
63 Simmons (2009) showed that less saltwater intrusion is expected when the system is
64 recharge-limited (flux-controlled). Unsurprisingly, the degree of land surface inundation
65 was found to control the amount of saltwater intrusion ([Behzad-Ataie-Ashtiani](#) et al.,
66 2013), and the impact of sea level rise on saltwater intrusion is enhanced by groundwater
67 extraction from coastal wellfields (Bobba, 2002; Langevin and Zygnerski, 2013).

68 Models of storm surge overwash events have been developed to evaluate their
69 impact on the freshwater lens. Most of these models used codes that neglect the surface
70 domain. However, Yang et al. (2013) used a fully-coupled subsurface and surface
71 approach that simulated tidal activity, coastal flow dynamics, and a hypothetical storm
72 surge on a coastal aquifer. All models indicate initial salt contamination of the freshwater
73 lens, which recovers to fresh concentrations over time due to ~~fresh-water~~freshwater
74 recharging at surface and density-driven downward migration of salt water (Terry and
75 Falkland, 2010). The occurrence of multiple storm surges (Anderson, 2002) and
76 accumulations of salt water at the surface in low depressions (Chui and Terry, 2012) may
77 increase the time for recovery of the lens. Where the vadose zone becomes thinner under
78 conditions of sea level rise (because the freshwater lens has risen in the subsurface), the
79 impact of storm surge alongside sea level rise may result in less salt contamination of the
80 freshwater lens (Chui and Terry, 2013). However, the salt contamination that does occur
81 under sea level rise conditions remains close to the surface of the lens (Terry and Chui,
82 2012). Wider islands generally result in less freshwater lens contamination than narrow
83 islands, as a result of their thicker lens morphology (Chui and Terry, 2013).

84 Although many aspects of climate change impacts on freshwater lenses have been
85 modeled previously, few studies have investigated both the spatial and temporal response
86 of the freshwater lens to the stressors. Climate change related stressors operate at various
87 spatial and temporal scales: island-wide impacts due to sea level rise and changes in
88 recharge occur over long time periods, on the order of decades, whereas local-scale
89 impacts due to storm surge overwash occur over short time periods, on the order of days.
90 This study evaluates the spatial and temporal response of an island freshwater lens to
91 various climate change stressors using a numerical modeling approach. To account for
92 the varying temporal and spatial scales of the stressors, two different density-dependent
93 flow and transport modeling codes are used. SEAWAT (Langevin et al., 2007) models
94 were developed at an island scale to simulate long-acting stressors, including sea level
95 rise and change in recharge. HydroGeoSphere (Therrien et al., 2010) models were
96 developed at a local scale to simulate storm surge which is a short-acting stressor. The
97 study aims to identify critical factors and stressors that may affect freshwater resources of
98 small, low-lying islands using Andros Island in The Bahamas as a representative island.
99 The results of the study are intended to be applicable to other islands with similar
100 hydrogeological settings.

101 **2. Site Description**

102 The study site is Andros Island in The Bahamas. Andros Island has undergone
103 limited development and groundwater exploitation; therefore, the hydrogeological data
104 collected in the 1970s (Little et al., 1973) are considered generally representative of
105 current conditions and can be used for baseline model calibration. Andros Island is
106 representative of other low-lying carbonate islands with thin freshwater lenses commonly
107 found throughout the Caribbean and ~~South~~-Pacific regions (Falkland, 1991; Vacher and
108 Quinn, 1997).

109 Andros Island is the largest island in The Bahamas, and is located ~~approximately~~
110 200 km southeast of Florida (Figure 1). It is ~~approximately~~ 14,000 km² in area and is

111 comprised of several smaller islands and cays. The highest elevation on the island is 20
112 metres above sea level (masl) along a ridge that parallels the east coast, whereas lower
113 elevations (< 1 masl) are common towards the west. The western coastline is largely
114 composed of wetlands and saltwater marshes, and therefore, ~~the majority of most~~
115 settlements are ~~situated~~ along the east coast of the island (Figure 1). The remainder of the
116 island is largely covered in pine forest. There are no permanent surface water bodies on
117 the island.

118 **Insert Figure 1**

119 Andros Island is located on the Great Bahama carbonate bank (Figure 1). The
120 geology of the island is predominantly Pleistocene Lucayan Limestone Formation, which
121 is ~~approximately around~~ 40 m thick (Beach and Ginsburg, 1980). Discontinuity surfaces
122 (unconformities) within the limestone are present as layers of paleosols recurring in the
123 upper stratigraphy (Beach and Ginsburg, 1980). These layers represent episodes of sub-
124 aerial exposure and are largely concentrated within the top 20 m (Beach and Ginsburg,
125 1980; Boardman and Carney, 1997). Underlying the Lucayan is a cavernous, highly
126 karstic, and relatively more permeable unit termed the pre-Lucayan, which is present
127 from ~~approximately~~ 43 m below ground surface (mbgs) to at least 75 mbgs (Boardman
128 and Carney, 1997). The geology below this depth has not been observed as most studies
129 focus on the shallow, freshwater-bearing units; however, deposits of carbonates on the
130 Great Bahama bank are estimated to be up to 7 km thick (Cant and Weech, 1986).

131 Due to its large size, the freshwater lens on Andros Island represents the principal
132 source of natural ~~fresh water~~freshwater for The Bahamas. ~~The majority of Most~~ local
133 residents rely on the municipal potable water supply ~~system~~(having less than < 0.4 g/L
134 salt concentration), which extracts groundwater from the lens via 11 wellfields distributed
135 across the island (Figure 1). The local drinking water guidelines define potable water as
136 having salt concentrations of less than 0.4 g/L. The largest of these wellfields is the North
137 Andros Wellfield. As is common with many freshwater lenses, there is potential for

138 upconing of the underlying saltwater and degradation of the lens if wells are deep and the
139 lens thin (Werner et al., 2009; White and Falkland, 2010). Therefore, the wellfields on
140 Andros employ horizontal trench-based groundwater extraction or a series of
141 interconnected shallow boreholes pumped at low rates. Typical depth of the wellfields is
142 between 1 and 5 mbgs. Water flows within the trench-based wellfields under a very low
143 gradient, towards a central low sump where water is pumped to storage reservoirs.

144 The hydrogeology of Andros Island is based on previous studies, most of which
145 were conducted around the wellfields and other developed areas. The principal aquifer is
146 | the unconfined Lucayan Limestone as the older (deeper) geological units are too
147 | permeable and thus are not able to prevent ~~fresh-water~~freshwater from mixing with the
148 surrounding saltwater (Cant and Weech, 1986; Schneider and Kruse, 2003). Soil zones
149 are sparse, and minimal runoff occurs during precipitation events (Little et al., 1973;
150 Tarbox, 1987). The freshwater lens is recharged solely through infiltrating precipitation,
151 which generally occurs during the wet season from May to October (Bukowski et al.,
152 1999). Average annual precipitation in the south is 39% less than average annual
153 precipitation in the north of Andros Island (Cant and Weech, 1986; Bahamas Department
154 of Meteorology, Climate Averages 1979-2000). Based on resistivity surveys conducted in
155 the north of the island, the thickness of the freshwater lens ranges from 3 to 20 m (Wolfe
156 et al., 2001); however, previous studies cite the maximum thickness as 34 m (Cant and
157 Weech, 1986) and borehole salinity profiles indicate the maximum thickness of the lens
158 is up to 39 m (Little et al., 1973). The lens is generally shallower in the southern regions
159 of Andros Island compared to the northern regions, with a measured thickness of at least
160 15 mbgs (personal communication, municipal water supply managers, Bahamas Water
161 and Sewerage Corporation). The elevation of the lens inland is approximately 2 masl
162 | (Ritzi et al., 2001) with typical depth to water of ~~approximately~~ 1-2 mbgs, although it is
163 deeper (up to 5 mbgs) under the high topography ridge along the east coast (Little et al.,
164 1973; Boardman and Carney, 1997). The hydraulic conductivity of the principal aquifer
165 (Lucayan Limestone) is estimated to range from 86 to 8,640 m/day based on short
166 duration, single-well specific capacity pumping tests conducted in the 1970s (Whitaker

167 and Smart, 1997). The hydraulic gradient (ranging from 0.0005 to 0.001) was determined
168 from historic field observations and estimates of the freshwater lens morphology (Little et
169 al., 1973). Porosity ranges from 10-20% (Bukowski et al., 1999). Sparse hydrogeological
170 field data are available for the majority of the island; therefore, in the past, the
171 morphology of the freshwater lens was largely inferred based on vegetation patterns,
172 geological setting and anecdotal observations. Because Andros Island is composed of
173 several small islands and cays, the freshwater lens is also composed of multiple lenses
174 present on the different land masses. Lenses are anticipated to be present across most of
175 the island, except in areas that are heavily intersected by saltwater marshes and wetlands.

176 In September 2004, Hurricane Frances caused a storm surge on the west coast of
177 Andros Island, which resulted in extensive salinization of the North Andros Wellfield
178 (Figure 2). The hurricane ranged from a Category 4 to Category 2 on the Saffir Simpson
179 Hurricane Scale while it travelled across The Bahamas from the southeast to northwest
180 (Franklin et al., 2006). The surge occurred September 3-4, 2004, while Hurricane Frances
181 passed near Andros Island. The exact time of occurrence of the storm surge and the actual
182 extent of the overwash are unknown because the western coast of Andros Island is largely
183 unpopulated. However, after the hurricane had passed, evidence of the overwash was
184 observed, such as flooded ground and the presence of marine fish at inland locations
185 (Bowleg and Allen, 2011). The likely extent of the overwash is thus based on
186 observations of damage following the surge (e.g. water marks on trees, presence of
187 seaweed and marine organisms, etc.) and is shown on Figure 2.

188

Insert Figure 2

189 Salinity concentration data from the southern wellfield (Figure 2) were provided
190 from the water managers for the dates: May 2004 (pre-storm), September 7th
191 (immediately post-storm surge), September 15th (following remedial action) and
192 July/August 2005 (approximately one year post-storm surge). These data are presented on
193 Figure 3, which illustrates the abrupt increase in salinity within the trenches following the

194 storm surge and the eventual recovery to pre-storm concentrations. As a form of remedial
195 action, the contaminated trenches were pumped to remove the ponded seawater beginning
196 on September 8th (approximately 4 days following the storm surge). Salinity in the
197 affected trenches improved, reducing by up to 88% on September 15th, relative to the
198 maximum recorded concentrations in each trench. However, remedial pumping of the
199 trenches was not completed because ~~fresh-water~~freshwater was required to support post-
200 hurricane relief efforts on other islands. Therefore, some of the contaminated trenches
201 were closed off from the wellfield system to allow for extraction of ~~fresh-water~~freshwater
202 from the unaffected parts of the freshwater lens and were not drained. Several of these
203 contaminated trenches remained closed for two years due to poor water quality. Trenches
204 that were drained are distinguished from those that were not in Figure 3. The wellfield
205 eventually recovered to normal salinity concentrations between one and two years post-
206 storm, with all trenches recovered by 2009.

207

Insert Figure 3

208 **3. Methodology**

209 **3.1 SEAWAT Model: Long-Acting Stressors**

210 *3.1.1 Baseline Model Setup*

211 A three-dimensional numerical density-dependent groundwater flow and solute
212 transport model was developed using SEAWAT. The island was simulated using two
213 separate models, a northern and southern model, to allow for refined grid resolution and a
214 reasonable run time for each simulation. Each model was run for 100 years during which
215 time the freshwater lenses developed; both models reached steady state (i.e. no further
216 change in lens morphology) within 20-25 years. Specified head boundaries were defined
217 along the perimeter of the domain to simulate sea level, with density specified at 1.025
218 kg/L, representative of typical seawater composition. Specified concentration boundaries

219 were assigned to the same grid cells as the specified head boundaries with concentrations
220 of 35 g/L salt. The initial concentration of the entire model domain was specified at 35
221 g/L salt. The ground surface for the model was based on a digital elevation model for
222 Andros Island (90 m resolution). The model grid was uniform in plan-view with each
223 grid cell ~~approximately~~ 500 m by 500 m. In the vertical dimension, the model included
224 44 layers, with individual layer thicknesses of 1 m in the upper 20 m of the model
225 domains, which transitioned to 2.5, 5 and then 10 m thickness from a depth of 60 m to the
226 base of the domain (200 mbgs).

227 Hydraulic conductivity of the principal aquifer was based on field data (Little et
228 al., 1973) and a sensitivity analysis was conducted to identify the optimal configuration
229 and hydraulic properties of the layers to simulate the observed freshwater lens thickness
230 on Andros Island. Previous studies had characterized the paleosols as low hydraulic
231 conductivity layers (Ritzi et al., 2001); however, anecdotal evidence indicates that the
232 layers are very weathered and may be highly conductive. In this study, the paleosols are
233 represented by relatively high hydraulic conductivity layers (interbeds) within lower
234 permeability limestone. This layer configuration with the assigned layer hydraulic
235 properties is supported by model calibration. Assigning a low conductivity to the
236 paleosols resulted in the lens being perched, which is not observed in the field. Whereas,
237 representing the paleosols as high conductivity layers within lower conductivity
238 limestone resulted in thin lenses being developed, similar to field observations. This
239 approach is consistent with other studies based in The Bahamas, which have suggested
240 that layers of high hydraulic conductivity in the subsurface are responsible for thin
241 freshwater lenses (Wallis et al., 1991). The optimal configuration of aquifer layers and
242 hydraulic conductivities are provided in Table 1.

243 Recharge was applied to the top layer of the model with concentration of 0 g/L
244 salt to simulate the average annual recharge to the aquifer. Recharge is the only input of
245 ~~fresh-water~~freshwater to the hydrogeological system and, therefore, is the main
246 mechanism by which the simulated freshwater lens develops in the model. The annual

247 recharge amount for Andros Island was estimated using the United States Environmental
248 Protection Agency's software HELP (Hydrologic Evaluation of Landfill Performance)
249 (Schroeder et al., 1994). HELP utilizes a storage routing technique based on hydrological
250 water balance principles. It accounts for soil moisture storage, runoff, interception, and
251 evapotranspiration. HELP has been used to estimate recharge for a variety of climatic and
252 physiographic settings (Scibek and Allen, 2006; Jyrkama and Sykes, 2007; Toews and
253 Allen, 2009; Allen et al., 2010).

254 Within HELP, a representative vertical percolation profile was defined for the
255 unsaturated zone. The depth of the profile was 2 m, based on a sensitivity analysis using
256 the minimum and maximum observed depths to the water table on Andros Island. No soil
257 zone was specified due to the generally thin/absent soils on Andros Island (Little et al.,
258 1973). The lithology was homogeneous (representing limestone), with a saturated
259 hydraulic conductivity (864 m/day) based on the mean value from field studies (Little et
260 al., 1973) and the calibrated value from the baseline SEAWAT model. Vegetation cover
261 was assigned to the highest class in the software (a leaf area index of 5) based on the
262 large proportion of pine forests. The surface was assigned zero slope given that minimal
263 runoff is observed. The wilting point was assigned 0.05 and field capacity 0.1 in the
264 absence of measured values.

265 Two 100-year climate data series were generated using the embedded stochastic
266 weather generator; one for North Andros and one for South Andros because the historical
267 climate differs between the two regions. The average annual precipitation on North
268 Andros is 1,442 mm/yr, while on and South Andros it is 889 mm/yr. Temperature
269 averages were not available for South Andros, therefore the monthly averages for North
270 Andros were applied to both models. Other climate parameters (e.g. windspeed and
271 relative humidity) were identical for both models. The historical statistical parameters for
272 climate were based on values for the nearest climate station (Miami, Florida, USA) in the
273 weather generator database.

274 The average annual recharge for the north was estimated at 877 mm/year, with a
275 minimum monthly average of 24 mm/month in December and a maximum monthly
276 average of 163 mm/month in August. The average annual recharge for the south was
277 estimated at 426 mm/year, with a minimum monthly average of 17 mm/month in
278 February and a maximum monthly average of 70 mm/month in October. These values
279 were used as input for the northern and southern SEAWAT models, respectively.

280 The hydrogeological parameters assigned to the SEAWAT model, based on field
281 data and sensitivity analyses, are summarized in Table 1. Storage parameters were based
282 on common values for the aquifer lithology (Younger, 1993). The wellfields were not
283 simulated in the baseline model in order to represent natural historical conditions. Given
284 their small size, The presence of the wellfields are is not anticipated to affect the
285 freshwater lens response due to their small area. If the system were head-controlled,
286 however, at a local scale, the rise in water table could result in more loss of freshwater
287 from the top of the lens. if the system were head-controlled.

288 **Insert Table 1**

289 **3.1.2 Climate Change Simulations**

290 Future climate for this study was based on published climate change projections
291 for The Bahamas (United Nations Development Programme (UNDP), 2010). The
292 projections were derived from 15 global climate models (GCMs) simulating three
293 emissions scenarios (SRES A2, A1B, and B1). Summaries of projected changes were
294 compiled as seasonal shifts for three-month groupings (McSweeney et al., 2010). For
295 each grouping, a range in values (minimum, median, and maximum) for each emissions
296 scenario were provided for the 2030s, 2060s and 2090s. The median seasonal shift in
297 temperature and precipitation projected for the 2090s for the A2 scenario (expected to
298 result in the greatest change) was selected for Andros Island, as summarized in Table 2.
299 Average daily temperature for the 2090s is projected to increase during all seasons
300 (between 2.8-3.2°C). Changes to precipitation are projected to occur primarily during the

301 summer (up to 42% reduction relative to current conditions). Overall, the projected
302 climate shifts represent conditions with less precipitation and higher temperatures - a
303 drier and hotter climate state.

304

Insert Table 2

305 Changes to groundwater recharge were determined by re-modeling recharge in
306 HELP using the projected 2090s climate. The seasonal climate shifts (applied evenly to
307 each month according to season) were applied to the monthly normals for temperature
308 and precipitation in the weather generator, and a new stochastic weather series was
309 generated to represent the projected future climate. This approach is consistent with that
310 used in other studies (e.g. Scibek and Allen, 2006). The adjusted climate data series was
311 then used as input to the vertical percolation profile to determine the annual average
312 groundwater recharge expected under projected climate change. As in the baseline
313 recharge modeling, recharge estimates were produced for North and South Andros, and
314 these values were applied to the SEAWAT models for each region, respectively. The
315 predicted average annual recharge for the north was 777 mm/year, with a minimum
316 monthly average of 18 mm/month in March and a maximum monthly average of 130
317 mm/month in August. The predicted average annual recharge for the south was 360
318 mm/year, with a minimum monthly average of 4 mm/month in July and a maximum
319 monthly average of 82 mm/month in November.

320 Sea level rise was simulated by increasing the elevation of the specified head
321 boundaries in the model domain. Loss of land surface due to inundation associated with
322 sea level rise was not simulated, as the grid resolution of the model is larger than the
323 inundation anticipated based on ground surface elevation. Therefore, the boundaries at
324 the edge of the model domain are anticipated to remain at the same model grid cell, only
325 representing a higher specified head value. Although sea level rise has been already
326 observed over the last several decades (White et al., 2005), there is uncertainty as to the
327 rate that it will occur in the future (Rahmstorf, 2007). Geographic variability in the rates
328 of sea level rise is also expected (White et al., 2005). Therefore, a predicted mean sea

329 level increase of 0.6 m by the 2090s (relative to 1980) was selected as an average
330 estimate based on global and regional projections of sea level rise (IPCC, 2007;
331 Rahmstorf, 2007; Obeysekera, 2013). The hydrogeological system of Andros Island is
332 considered recharge-limited rather than topography-limited, because there is some
333 capacity for the freshwater lens to rise in the unsaturated zone without leading to surface
334 flooding (Werner and Simmons, 2009).

335 Both the reduction in recharge and sea level rise were simulated in the models as
336 incremental instantaneous shifts. Three models were run: one for recharge reduction
337 alone, one for sea level rise alone, and one including both stressors. The baseline model
338 was run for 50 years to allow the freshwater lens to develop. The recharge and specified
339 head boundary values were then adjusted every 10 years until reaching the projected
340 values for the 2090s. This assumes uniform rates of change throughout the 100 year
341 simulation.

342 Observation wells were defined in the models to capture a discrete record of
343 simulated concentration for every time step. The observation wells were located within
344 the center and at the edge of the freshwater lens to represent areas that are anticipated to
345 be, respectively, most resilient and most vulnerable to stressors. The northern model
346 consists of one landmass and, therefore, one principal lens, whereas the southern model
347 consists of multiple landmasses. As discussed below, two principal lenses form in the
348 southern model. Therefore, two observation wells were assigned in the northern model
349 and four observation wells were assigned in the southern model, representing central and
350 peripheral wells for each anticipated freshwater lens. The wells are identified as A and B
351 to distinguish between the two principal lenses in the southern model. Each well was
352 screened from the ground surface to at-5 mbgs, corresponding to the maximum depth of
353 most wells/wellfields on Andros Island.

354 In order to evaluate changes to the freshwater lens morphology in response to
355 climate change, the SEAWAT model island-scale results were quantitatively evaluated

356 using a geographic information system (GIS). The volume and area of the lens were
357 calculated based on a threshold salt concentration 0.4 g/L or less (representing local
358 potable water guidelines) and porosity, which effectively corresponds to total dissolved
359 solids (Guo and Langevin, 2002). Although there are inaccuracies inherent in this
360 approach, it provides an estimate of the lens morphology that ~~This approach allowed~~ for
361 quantitative comparison of the changes in freshwater lens morphology between different
362 stressors applied in the island-scale model. This threshold concentration is based on the
363 water quality guidelines for salinity in the municipal supply on Andros Island. It also falls
364 within common definitions of ~~fresh water~~ freshwater containing less than 1.0 g/L of total
365 dissolved solids (Freeze and Cherry, 1977; Barlow, 2003). The World Health
366 Organisation (WHO) drinking-water guidelines do not stipulate a maximum threshold for
367 salt in water, except as it relates to unacceptable taste. The WHO recognizes that water
368 that tastes fresh often has a salt concentration of less than 0.25 g/L; however, in regions
369 where there is naturally more salt in the water there may be a higher taste threshold
370 (WHO, 2011).

371 **3.2 HydroGeoSphere Model: Short-Acting Stressor**

372 Modeling the impact of storm surge overwash on a hydrogeological system
373 involves simulating density-dependent flow and solute transport across the surface, the
374 vadose zone and the saturated domain. HydroGeoSphere (HGS) was identified as the
375 most suitable tool to simulate these coupled processes because it is a fully integrated
376 surface and variably saturated subsurface model that is capable of simulating these
377 processes across all domains. By solving the surface and subsurface flow equations
378 simultaneously, HGS provides more realistic representations of the major processes than
379 simpler or independently coupled models (Goderniaux et al., 2009).

380 One of the mechanisms of aquifer contamination following storm surge is from
381 open wells or trenches that provide direct access to the water table and collect the salt
382 water during inundation (Terry and Falkland, 2010). In addition, salt water trapped within

383 a borehole, or other direct pathway into the aquifer, may lead to prolonged release of salt
384 water into the surrounding aquifer over time (Illangasekare et al., 2006). These features
385 may delay recovery of the aquifer and, therefore, are an important component to include
386 in modeling studies of storm surge impacts (Chui and Terry, 2013). Major consequences
387 to water supply are likely to result when storm surge waves strike trench-based wellfields
388 or open boreholes, as occurred on Andros Island in 2004. Notwithstanding this risk,
389 trench-based wellfields are commonly used on low-lying islands to limit upconing. The
390 models developed for this study aim to characterise aquifer damage and recovery from a
391 storm surge overwash, specifically in the context of a trench-based wellfield and the
392 impact on water supply.

393 The model domain represents a highly discretized, two-dimensional cross-section
394 of one of the trenches in the North Andros Wellfield (Figure 4). The size of the model
395 domain had to be made as small as possible for computational reasons. Therefore, several
396 different model configurations were tested by varying the model domain width and the
397 hydraulic conductivity distribution (limestone and paleosols) to identify the optimal
398 combination of parameters that best approximates observed conditions. The physically-
399 based seawater boundaries are important components in simulating flow within a
400 freshwater lens. In reality, these boundaries are located along the coastline; however, the
401 coastline is far from the North Andros Wellfield. Therefore, local-scale models were
402 developed using boundary conditions assigned in such a way as to simulate a realistic
403 flow field surrounding the trench. The local-scale models were calibrated based on
404 critical factors that are expected to affect freshwater lens contamination and recovery.
405 These critical factors include: recharge, thickness of the vadose zone, aquifer hydraulic
406 conductivity, geological heterogeneity (e.g. paleosols), water table gradient, and
407 thickness of the freshwater lens. Field data for each of these factors (as presented earlier)
408 comprise the calibration criteria as summarised in Table 3.

409

Insert Table 3

410 With increasing model domain width, the elevation of the water table and gradient
411 both increase, whereas the thickness of the lens decreases. The opposite response was
412 observed when hydraulic conductivity was increased. The model setup that satisfied the
413 calibration criteria with the smallest domain width was selected as the baseline model for
414 this study (Figure 4).

415 The model uses block elements that range from 0.35-1.0 m. Grid refinement was
416 done in order to optimise simulation of flow and transport across the three hydrologic
417 domains and to allow for the evaluation of small-scale changes in response to overwash.
418 The model domain covers a horizontal extent of 2400 m and a vertical extent of 43.5 m,
419 with sea level assumed to be 3.5 mbgs. The vertical extent of the domain was determined
420 to represent the Lucayan Limestone. The model domain was 1 unit thickness, with a
421 uniform horizontal grid spacing of 1 m. Vertical grid refinement varied from 1 m thick in
422 the lower 20 m, to 0.5 m thick in the overlying 20 m, and 0.35 m thick in the uppermost
423 3.5 m. Paleosols were simulated in the subsurface as 1 m thick zones at 9 and 14 mbgs
424 (corresponding to field observations). The hydraulic conductivity was defined as
425 isotropic at 86.5 m/day for ~~the portion of the~~ ~~the majority~~ ~~all of the~~ domain (representing
426 the Lucayan Limestone) and 865 m/day for the paleosols. The hydraulic conductivities lie
427 within the observed range, although they are lower than that used in the SEAWAT model
428 in order to calibrate the FWL-freshwater lens morphology at the local-scale surrounding
429 the trench. The underlying high conductivity pre-Lucayan limestone was not included in
430 the model as it was observed to not have a significant impact on the freshwater lens
431 morphology at the scale of the model.

432 The trench itself extends 2 mbgs, intersecting the top of the water table. Most
433 trench-based wellfields rely on gravity flow; therefore, water tends to move very slowly
434 within the trenches and is observed to be almost stagnant unless the trench is actively
435 being drained. Therefore, lateral flow within the trench was assumed to have a negligible
436 impact on the storm surge impact and recovery of the aquifer. The model provides a

437 snapshot of the impact of trench-based wellfields in terms of salt water capture and
438 transport into the aquifer, which may be scaled up to represent the whole wellfield.

439

Insert Figure 4

440 Specified head with associated concentration boundaries were assigned to both
441 sides of the model to represent the surrounding seawater (Figure 4). Recharge was
442 applied to the surface domain as an annual average quantity based on the HELP recharge
443 modeling, presented earlier. Recharge provides the only input of ~~fresh-water~~freshwater
444 that enables the freshwater lens to develop. The boundary conditions and hydrogeological
445 parameters assigned to the HGS model are summarized in Table 4.

446

Insert Table 4

447 The simulation of storm surge overwash required three separate modeling phases:
448 1) development of the freshwater lens to steady state conditions; 2) short temporal-scale
449 modeling of the rise in salt water height accompanying the overwash; and 3) recovery of
450 the freshwater lens. The heads and concentrations at the end of each phase are used as
451 initial conditions for the subsequent phases; however, the boundary conditions are
452 changed to reflect the different scenarios. The three phases are required to accommodate
453 the different temporal scales (i.e. decades for lens development and minutes for storm
454 surge occurrence) as well as to assign the time-varying boundary conditions. ~~Most-All~~
455 model simulations used the same initial steady state freshwater lens (Phase 1) and
456 simulation of the storm surge overwash (Phase 2). Different scenarios of remedial action
457 were simulated for Phase 3 and compared to the baseline recovery scenario.

458 **Phase 1: Freshwater Lens Development**

459 Phase 1 is a model spin-up period during which the freshwater lens develops. The
460 initial concentration in the baseline model domain was salty (35 g/L), with the only

461 | source of ~~fresh water~~ freshwater being recharge. The model was run for 50 years to reach
462 steady state.

463 **Phase 2: Storm Surge Inundation**

464 Phase 2 simulates the occurrence of a storm surge overwash event. The surface
465 domain was inundated with up to 1 m of water, based on observations following the 2004
466 storm surge on Andros Island. Flooding was simulated at a gradual rate of 0.1 m per 10
467 minute stress period to satisfy model convergence criteria. Once full inundation was
468 reached (1.5 hours after start of flooding), the maximum flood level was held constant for
469 2 hours. The actual period of inundation is not known, so this period was estimated to
470 allow for sufficient salt water to enter the system. The salt concentration of the flood
471 water was assigned as 35 g/L to represent seawater.

472 **Phase 3: Recovery of the Freshwater Lens**

473 Phase 3 involved simulating the recovery of the freshwater lens. Several different
474 scenarios were tested to enable comparison of recovery times when different factors are
475 varied. All scenarios are based on the output from Phase 2, with the head and
476 concentration boundaries of the surface domain unconstrained to allow release of the
477 salty flood water. All other boundaries remained the same as the initial Phase 1 model.

478 A baseline recovery scenario was simulated for 10 years following the storm
479 surge to allow the salt water to be flushed out of the system under the influence of
480 recharge. In the baseline recovery model, the freshwater lens returns naturally to its
481 original morphology.

482 Several other scenarios were simulated to represent different remedial actions.
483 Following a storm surge event when the trenches are filled with salt water, a common
484 remedial action is to drain out the trenches to remove the captured salt water
485 (Illangasekare et al., 2006; Terry and Falkand, 2010; Chui and Terry, 2012). Draining, or

486 pumping out the trenches, is meant to improve the recovery time and assist with removal
487 of the salt water from the system. However, draining may often be delayed due to access
488 constraints or due to lack of coordination and emergency response following the storm
489 surge. Therefore, models were developed where the trenches are drained at different
490 times and for different durations to evaluate the impact of draining protocol on recovery
491 times of the freshwater lens and impact to water supply. Scenarios were modeled
492 whereby draining was delayed by one, two, three, or four days after the storm surge (to
493 reflect a delay in action). Other scenarios modeled draining initiated one day after the
494 storm surge, whereby the duration of draining was one, two, or three days (to investigate
495 the effect of sustained periods of draining).

496 For all recovery simulations, observation points were assigned within and
497 immediately below the trench to monitor salt concentrations during recovery. This
498 allowed for the comparison of recovery times between different scenarios, specifically
499 the number of days for potable water to return to the trench and aquifer.

500 **4. Results**

501 **4.1 Long-Acting Stressors**

502 *4.1.1 Baseline Model*

503 The simulated freshwater lens in the baseline model provides a snapshot of the
504 average annual freshwater lens morphology. The model results indicate that a ~~thin~~-lens is
505 present throughout most of the model domain (not shown); however, this study focuses
506 on areas considered viable to provide a sustainable water supply, which are defined as
507 having a lens thickness of greater than 2 m and concentration less than 0.4 g/L (Figure 5).
508 The shape of the lens is relatively symmetrical in cross-section with an average hydraulic
509 head of 1.8 masl, which corresponds to typical elevations observed of 2 masl. The
510 estimated total area of the viable freshwater lens on Andros Island is ~~approximately~~
511 around 2,000 km² with a freshwater volume of ~~35.93~~ $35.93 \times 10^{10} \text{ m}^3$.

512

Insert Figure 5

513 The baseline model was calibrated to observations, where available, although
514 these were sparse and based on varying time periods (from the 1970s to early 2000s). The
515 extent of the lens generally corresponds to observations of freshwater occurrence (i.e. the
516 presence of wells and wellfields) and the results of previous studies (Little et al., 1973;
517 Cant and Weech, 1986; Wolfe et al., 2001). The freshwater lens in the northern model is
518 composed of a single lens that is much larger than the smaller, separate lenses in the
519 southern model. Along the coastlines, particularly in the southern regions of the island,
520 the simulated freshwater lens tends to be situated further inland than is observed;
521 however, the depth of the simulated lens in the south is consistent with field observations.
522 The depth of the simulated lens in the northern regions of Andros Island falls within the
523 range of maximum observed lens depth (up to 39 mbgs), although it is slightly deeper
524 than typical observations of around 15 to 20 mbgs. Because most of the model
525 parameters are based on field data and sensitivity analyses, the deeper simulated lens is
526 likely the result of slight over-estimation of recharge in the HELP model. HELP applies
527 daily precipitation to the lithology profile evenly over a 24 hour period, when in reality,
528 precipitation events occur within shorter time intervals (hourly) and leads to some pooled
529 water on the ground surface. Given that the intensity of the precipitation events is not
530 accounted for in HELP, the resulting recharge estimates may be slightly over-estimated.
531 However, there is no clear basis upon which the recharge estimates can be adjusted to
532 achieve better model calibration due to the lack of field data for actual evapotranspiration
533 and recharge.

534 Some local-scale variations are neglected in the model due to the limitations of
535 the large grid cell size required to cover the area of the island, which resulted in a low
536 resolution of the ground surface elevation. In addition, the model was developed to
537 represent the average annual freshwater lens morphology and, therefore, does not include
538 seasonal variation. Although the worst case scenario (e.g. lowest recharge during the dry
539 season) is not accounted for in this study, other studies have shown that there is little

540 seasonal variation in groundwater levels for islands of similar hydrogeological setting
541 (Momi et al., 2005). Overall, the simulated lens is within the range of observed depths,
542 although it represents a slight over-estimation of the freshwater resources in the northern
543 region of Andros Island. The model provides a generalized estimate of the freshwater
544 lens morphology and serves as a reasonable baseline for investigating the impacts due to
545 climate change stressors.

546 *4.1.2 Climate Change Models*

547 As noted above, the HELP model utilizes site-specific climate averages so that
548 predictions can be made regarding the impact of future climate conditions on recharge.
549 Recharge is projected to decrease by 11% in the northern model and decrease by 15% in
550 the southern model by the 2090s relative to baseline (current) recharge. This is due
551 largely to decreases in average annual precipitation, and slight increases in
552 evapotranspiration rates. Minimal changes in soil storage were simulated in the HELP
553 model.

554 The results of the climate change modeling, including a reduction in recharge and
555 a rise in sea level, indicate that the freshwater lens will reduce in areal extent and volume
556 under future climate change conditions. The percent change in freshwater lens area and
557 volume relative to the baseline values are presented in Table 5. The change in area and
558 volume of the lens indicate that the lens shrinks and thins in response to the stressors. For
559 both the northern and southern models, simulations of reduced recharge alone result in
560 the majority of freshwater lens reduction, with sea level rise contributing a smaller
561 proportion of lens reduction. ~~In the southern model, the results indicate a 19% volume~~
562 ~~loss due to reduced recharge compared to 5% volume loss due to sea level rise relative to~~
563 ~~baseline morphology.~~ ~~Overall, †~~The freshwater lens in the southern model is predicted to
564 incur a greater percentage of loss of lens compared to the northern model under climate
565 change conditions. In the southern model, the results indicate a 19% volume loss due to
566 reduced recharge compared to 5% volume loss due to sea level rise relative to baseline

567 | morphology. Whereas, in the northern model, 5% of volume loss is due to reduced
568 | recharge with 0.9% volume loss due to sea level rise. The simulated lens at the end of the
569 | 100 year simulation is presented, illustrating areal loss of lens relative to the baseline
570 | model (Figure 6).

571 | **Insert Table 5**
572 | **Insert Figure 6**

573 | The simulated time-varying dissolved salt concentrations in the observation wells
574 | are shown in Figure 7. The simulated concentrations at most observation wells indicate
575 | that salinity in the lens progressively increases in response to the climate change shifts
576 | applied every 10 years starting at 50 years. Prior to 50 years, the model is spinning up
577 | from a fully salty state. Dissolved salt concentrations in all of the observation wells reach
578 | near steady state between stress periods (only very small changes continue to occur on
579 | the order of 10^{-10} g/L per day). The time to reach steady concentrations is relatively
580 | similar in all wells, ranging from 0.5 to 3 years and increasing as the simulation
581 | progresses. This indicates that even though the climate change shifts in each stress period
582 | are the same magnitude, the freshwater lens takes longer to adjust to the shifts as the
583 | cumulative magnitude of climate change increases.

584 | **Insert Figure 7**

585 | The central wells were placed in areas that were anticipated to be more resilient to
586 | stressors, and the peripheral wells ~~were located~~ in areas that were anticipated to be more
587 | vulnerable to stressors (thereby showing a more immediate lens thinning). The simulation
588 | results are consistent with the anticipated behaviour. The peripheral observation wells
589 | have higher dissolved salt concentrations than the central wells because they are situated
590 | in the thinner part of the freshwater lens, and therefore, are more likely to intersect the
591 | base of the lens. The highest dissolved salt concentrations are in the peripheral well in the

592 | northern model, which is ~~located~~ closer to the coast than the peripheral wells in the
593 | southern model. This is because the edge of the northern freshwater lens extends further
594 | coastward than the southern freshwater lens. Greater changes in dissolved salt
595 | concentration are also observed in the peripheral wells compared to the central wells, as
596 | ~~might would~~ be expected.

597 | **4.2 Short-Acting Stressor**

598 | **4.2.1 Freshwater Lens Development and Storm Surge Inundation**

599 | The morphology of the freshwater lens reaches steady state within 25 years at a
600 | maximum depth of 23 m below sea level (mbsl) (Phase 1; Figure 8a). The model is
601 | ~~calibrated to observed conditions meets the calibration criteria~~ outlined in Table 3. The
602 | maximum elevation of the freshwater lens is observed in the trench at 1.8 masl. The
603 | vadose zone surrounding the trench is approximately 1.7 m thick. The gradient across the
604 | model domain is 0.0015, with an average horizontal groundwater velocity of 0.87 m/day.
605 | The inflections on the sides of the lens at 9 and 14 mbgs reflect the high hydraulic
606 | conductivity paleosol layers.

607 | Simulation of storm surge inundation (Phase 2) resulted in high salt
608 | concentrations at the surface of the model up to 1 m above ground surface (Figure 8b).
609 | The results of the inundation model are shown for a focus area within 25 m of the trench
610 | (focus area indicated on Figure 8a). Within the 2 hour inundation period, the salt water
611 | had already been transported into the vadose zone due to the hydraulic gradient
612 | associated with the surface flood, and had also filled the trench with salt water (Figure
613 | 8b).

614 |

Insert Figure 8

615 | **4.2.2 Aquifer Recovery**

616 The baseline recovery of the freshwater lens (natural recovery) is shown for six
617 times post storm surge (Figure 9): 12 hours, 1 day, 2 days, 1 month, 2 years, and 10
618 years. The baseline recovery scenario indicates that the freshwater lens returns to its
619 original morphology approximately 10 years post storm surge. The salt water is
620 transported from the surface domain into the aquifer system, where it forms a salt plume
621 within the subsurface. This plume is flushed out over time due to the infiltrating
622 freshwater recharge. Salt concentration within the trench returns to levels below the
623 potable water threshold within 149 days following the storm surge for the baseline
624 recovery scenario.

625

Insert Figure 9

626 The results of the different draining scenarios are shown in Figure 10, alongside
627 the baseline recovery scenario, as relative concentration data over time, where 1.0
628 represents salt water and 0.0 represents ~~fresh-water~~freshwater. The number of days to
629 reach potable concentration in the trenches is indicated for each scenario. Observed
630 concentration data for the North Andros Wellfield trenches are also presented in Figure
631 10. Trenches that were drained following the storm surge, and those that were isolated
632 from the system and not drained, are distinguished by different symbols.

633 There is little difference in observed concentrations ~~between-when comparing~~ the
634 trenches that were drained and those that were not. The observed concentrations are
635 similar to the simulated concentrations immediately following the overwash event;
636 however, at one year post-storm surge, the observed concentrations are slightly above the
637 potable water threshold. By two years post-storm surge (not shown), the observed
638 concentrations are similar to the simulated concentrations, and below the potable
639 threshold.

640 Draining of the trenches generally results in a faster recovery. If draining occurs
641 within one day of the storm surge, potable water returns to the trench by about 120 days

642 (Figure 10), approximately one month sooner compared to the baseline recovery
643 simulation (149 days). With every day that draining is delayed, it takes longer for potable
644 water to return to the trench (corresponding to the small vertical lines on Figure 10 for
645 each scenario). After a delay of three days, the recovery time for potable water to return
646 is the same as the case when no remedial action is undertaken. Therefore, the
647 improvements in recovery time are dependent on the timing of draining.

648 In contrast, the duration of draining (not shown) does not significantly improve
649 recovery times. Draining that occurs for multiple days results in slightly longer times for
650 potable water to return compared to short-duration draining (i.e. over a single day).

651 **Insert Figure 10**

652 As mentioned earlier, the observed data at one year post storm surge are higher
653 than the model results, indicating that the trenches on Andros Island recovered slower
654 than the model results. This is likely the result of several factors:

655 1. The amount of salt water entering the aquifer system largely depends on
656 the time of inundation. As this was unknown, it was assumed as a two
657 hour inundation. However, the inundation may have lasted much longer as
658 no observations of the area were made until three days after the storm
659 surge. To account for this uncertainty, a Phase 2 model was run with a
660 longer inundation period of two days. The recovery from this storm surge
661 scenario took at least two months longer, with higher concentrations at one
662 year post-storm surge. However, the freshwater lens morphology
663 recovered at the same time as the baseline scenario.

664 2. ~~Another factor is t~~The amount of recharge that specifically occurred on
665 Andros Island may have been different during 2004-2005. Alternate
666 recovery simulations were run where recharge was applied as monthly
667 averages based on the 2004 and 2005 rainfall data for Andros Island.

668 These simulations resulted in longer recovery times, up to six weeks more
669 than baseline recovery.

670 3. As previously discussed, the HELP recharge results may over-estimate
671 actual recharge to the freshwater lens. Therefore, additional models were
672 run with recharge applied at half the baseline amount. These simulations
673 indicated that recovery was delayed by two months.

674 4. Additional factors may impact the calibration to observed data. The
675 models were developed based on field studies that were not all specific to
676 the North Andros Wellfield area; therefore, hydrogeological conditions
677 (such as porosity or hydraulic conductivity) at the wellfield may differ
678 from those at the island scale.

679 5. The exact timing, duration and method of draining utilised on Andros
680 Island are also unclear. While the best possible information was obtained
681 from the Bahamas Water and Sewerage Corporation, it is likely that the
682 details of operations were inexact.

683 6. Lastly, other hurricanes passed near to Andros Island in the weeks and
684 months following Hurricane Frances; however, it is unknown whether any
685 of these caused an additional storm surge event (National Hurricane
686 Center, National Oceanic and Atmospheric Administration (NOAA),
687 2014). Regardless, the close passage of other storms would have attributed
688 to atypical rainfall events. In addition, the concentration of recharging
689 freshwater may be higher than 0 g/L during storms due to salt spray,
690 thereby introducing higher salt concentrations at the surface and delaying
691 recovery.

692 Although many factors contribute to the uncertainty in the calibration, the
693 recovery models are likely reasonable representations that allow for comparison of the
694 impact of remedial actions on recovery.

695 **5. Discussion**

696 **5.1 Long-Acting Stressors**

697 The volume and area of the freshwater lens are reduced under scenarios of
698 stressed conditions, indicating that the lens both shrinks and thins. A significant impact is
699 observed in areas where the lens shrinks (i.e. along the periphery), as most settlements
700 and related infrastructure are typically near the coast on small islands, alongside a trend
701 in coastal migration of settlements (Ranjan et al., 2009; Cashman et al., 2010). As a
702 result, any changes in the freshwater lens morphology within the coastal zone may affect
703 access and availability of freshwater near the population centres.

704 The loss of freshwater lens area and extent under climate change conditions is
705 attributed more to the impact of changes to groundwater recharge than the impact of sea
706 level rise. Although loss of land surface due to sea level rise was not simulated in the
707 models, estimates based on ground surface elevation suggest loss of land surface (and
708 resulting loss of freshwater lens volume) is limited. On islands with lower topography
709 and/or smaller land area, inundation would have a greater effect on loss of freshwater
710 lens volume. These model results for Andros Island are supported by other studies,
711 which show that conditions of reduced groundwater recharge (or prolonged drought,
712 which results in reduced recharge) disturb the balance of freshwater outflow necessary to
713 maintain the extent and thickness of the freshwater lens, thereby leading to loss of
714 freshwater resources due to saltwater intrusion (Ranjan et al., 2009; White and Falkland,
715 2010; Mollema and Antonellini, 2013). In addition, the hydrogeological system on
716 Andros Island is recharge-limited, meaning that the freshwater lens is able to rise in the
717 subsurface in response to sea level rise. Therefore, it is less vulnerable to sea level rise

718 because the freshwater lens is able to maintain a balance between the hydraulic gradient
719 of the fresh and salt water (Michael et al., 2013). This assumption is only valid to a point;
720 for higher magnitudes of sea level rise, the freshwater lens would likely become
721 topographically-limited and, therefore, have a larger response (i.e. loss of lens) due to sea
722 level rise. Although sea level rise appears not to be a significant factor for saltwater
723 intrusion on Andros Island, it may increase the island's vulnerability to other events, such
724 as extreme high tides and storm surge overwash. These events have the potential to result
725 in significant impacts to the freshwater lens, as is discussed below.

726 The northern regions of Andros Island appear to be more resilient to climate
727 change stressors than the southern regions. Several factors contribute to the difference in
728 response between the northern and the southern regions: 1) the south is composed of
729 smaller landmasses, resulting in smaller areas for the freshwater lenses to develop; 2)
730 significantly less rainfall occurs in the south, meaning that there is less recharge to
731 sustain the freshwater lenses; and 3) lower recharge results in a thinner lens developing,
732 leading to lower hydraulic gradient of the freshwater lens~~the topography of the south is~~
733 ~~generally lower than that in the north, resulting in a slightly lower hydraulic gradient of~~
734 ~~the freshwater lenses~~. The combined impact of these factors is that the southern region of
735 Andros Island has smaller freshwater lenses that are more vulnerable to damage from
736 stressors.

737 The simulated freshwater lens on Andros takes longer to respond to climate
738 change stressors as the magnitude of the cumulative stress increases (i.e. lower recharge
739 and higher sea level). The implication is that as climate change progresses over time, the
740 ability of the freshwater lens to respond to these changes decreases. Because recharge is
741 the main driver of lens formation and maintenance, when the rate of recharge is reduced,
742 the response time of the hydrogeological system is also reduced. This has been observed
743 in laboratory experiments (Stoeckl and Houben, 2012), whereby the lens takes longer to
744 reach steady state when there is reduced input (i.e. specified flux or concentration
745 boundaries) to the system. Therefore, areas where there is less recharge, such as the

746 southern regions of Andros Island, are expected to take longer to react and adapt to
747 stresses to the hydrogeological system.

748 **5.2 Short-Acting Stressor**

749 Trench-based wellfields result in large salt plumes that develop in the aquifer
750 following a storm surge overwash. This is because the trench provides direct access for
751 inundating salt water to travel into the aquifer. The salt plume remains larger surrounding
752 the trench than in the rest of the aquifer throughout recovery, and takes 3 months longer
753 to recover than the surrounding aquifer. This is supported by other studies where it was
754 observed and modeled that areas where salt water pools or is collected during inundation
755 (such as open boreholes or depressions) result in longer recovery times (Terry and
756 Falkland, 2010, Chui and Terry, 2012).

757 The timing of remedial action (specifically draining of the trenches) is more
758 critical than the duration of draining. It is critical to drain the trenches as soon as possible
759 following a storm surge overwash in order to remove the initial salt load to the aquifer
760 before it is transported deeper into the aquifer. After a certain period of delay, there is no
761 improvement in recovery achieved by draining. This is illustrated in the simulation
762 results as well as the observation data, where there is little improvement in recovery for
763 trenches on Andros Island that were drained after a 4 day delay. The time of this delay
764 threshold, where there is still benefit to be gained in draining the trenches, will depend on
765 many factors, such as the hydraulic conductivity, the groundwater velocity, and recharge
766 rates. For most typical low-lying islands, the delay threshold is likely quite soon after
767 storm surge due to the high hydraulic conductivity of geological materials normally
768 found on low-lying islands (Ayers and Vacher, 1986). Coarser aquifer material may
769 allow for faster salt transport into the aquifer (Chui and Terry, 2012). Although this effect
770 may also speed up recovery, it means that there is a limited time in which to perform
771 remedial action to remove the salt water. On Andros Island, the delay threshold is 3 days.
772 The duration of draining should also be short, because longer durations of draining may

773 result in slower recovery times. This is likely due to the fact that draining of the trenches
774 removes the recharging ~~fresh water~~ freshwater, along with the salt water.

775 **6. Conclusions**

776 Stressors act over varying spatial and temporal scales to impact the freshwater
777 lenses of low-lying islands. Both short and long-acting stressors may result in significant
778 loss of freshwater resources. The model results are inherently uncertain due to
779 uncertainty associated with the input data, model conceptualisation, and stressor
780 scenarios. The greatest uncertainty lies in the simplification of the hydrogeology and the
781 associated parameters. This is largely due to limited studies having been conducted on
782 Andros. However, small islands often have limited capacity for hydrogeological
783 investigations. Therefore, this study was not predictive, but rather aimed to identify the
784 likely response based on the hydrogeological setting and the mean projected climate state
785 derived from multiple climate change model scenarios. To rigorously address uncertainty,
786 a series of models with a range of input parameters and climate scenarios would be
787 required–; however, this was beyond the scope of the current study. Within these
788 limitations, the results of the study provide the following conclusions~~The conclusions of~~
789 ~~this study are as follows:~~

790 1. The impacts of stressors on the freshwater lens are predicted to occur primarily
791 in areas where the freshwater lens is smaller or thinner, such as the periphery of the lens.
792 As most settlements are concentrated within the coastal zone, Most settlements and
793 related infrastructure are often located near to the coast on small islands, alongside a
794 trend in coastal migration of settlements (Ranjan et al., 2009; Cashman et al., 2010), and
795 therefore, even small-scale changes to the freshwater lens morphology in these areas may
796 have significant implications for freshwater sustainability.

797 2. Change to Ggroundwater recharge is identified as a key stressor to Andros
798 Island, where greater impacts to the freshwater lens are observed in areas with lower
799 recharge.

800 3. The response time of the freshwater lens (time to reach steady state) increases
801 as the magnitude of the stressors increase. With increasing magnitude of change to the
802 hydrogeological system, the freshwater lens takes longer to adjust to the new state.

803 4. The freshwater lens is generally able to recover from storm surge inundation
804 over time as fresh recharge flushes the salt plume out of the aquifer. Eventually, the
805 freshwater lens returns to the original morphology.

806 5. Trench-based wellfields may increase the potential storm surge impacts on the
807 freshwater lens, depending on the hydraulic conductivity, the vadose zone thickness-of
808 the vadose zone, and land cover. However, they also allow for ;however, remedial action
809 (such as draining the trenches) should-to be undertaken to-which can improve recovery
810 times. The sooner draining occurs, the more improvement in recovery, because, if
811 draining is delayed by too long (in this case, 3 days or more), there is no improvement in
812 recovery. The duration of draining has less effect on recovery and only needs to occur for
813 a short period of time.

814 **Acknowledgements**

815 Funding for this research was provided by the Natural Sciences and Engineering
816 Research Council (NSERC) through a Discovery Grant to Diana Allen, and a grant to
817 Simon Fraser University by The Nature Conservancy through the Royal Bank of
818 Canada's Blue Water ProjectTM. The authors also acknowledge the contribution of the
819 Bahamas Water and Sewerage Corporation in providing data for model calibration.

820 **References**

- 821 Allen, D.M., Cannon, A.J., Toews, M.W. and Scibek, J.: Variability in simulated
822 recharge using different GCMs, *Water Resour. Res.*, 46, W00F03,
823 doi:10.1029/2009WR008932, 2010.
- 824 Anderson, W.P. Jr.: Aquifer salinization from storm overwash, *J. Coastal Res.*, 18 (3),
825 413-420, 2002.
- 826 ~~Behzad, A.~~ Ataie-Ashtiani, B., Werner, A.D., Simmons, C.T., Morgan, L.K. and Lu, C.:
827 How important is the impact of land-surface inundation on seawater intrusion
828 caused by sea-level rise?, *Hydrogeol. J.*, 21, 1673-1677, doi 10.1016/
829 j.advwatres.2012.03.004, 2013.
- 830 Ayers, J.F., and Vacher, H.L.: Hydrogeology of an atoll island: A conceptual model from
831 detailed study of a Micronesian example, *Ground Water*, 24, 185-198, doi:
832 10.1111/j.1745-6584.1986.tb00994.x, 1986.
- 833 Barlow, P.M.: *Ground Water in Freshwater-Saltwater Environments of the Atlantic*
834 *Coast*, U.S. Department of the Interior, US Geol. Surv., Circular 1262, Reston,
835 Virginia, USA, 2003.
- 836 Beach, D.K., and Ginsburg, R.N.: Facies succession of Pliocene-Pleistocene carbonates,
837 northwestern Great Bahama Bank, *AAPG Bull. -Am. Assoc. Petr. Geol.*, 64(10),
838 1634-1642, 1980.
- 839 Bear, J., Cheng, A.H.D., Sorek, S., Herrera, I. and Ouazar, D. (Eds.): *Seawater Intrusion*
840 *in Coastal Aquifers*, Kluwer Academic Publishers, Dordrecht, The Netherlands,
841 1999.
- 842 Biasutti, M., Sobel, A.H., Camargo, S.J., Creyts, T.T.: Projected changes in the physical
843 climate of the gulf coast and caribbean. *Climatic Change*, 112(3-4), 819-845, doi:
844 10.1007/s10584-011-0254-y, 2012.
- 845 Boardman, M.R., and Carney, C.: Influence of sea level on the origin and diagenesis of
846 the shallow aquifer of Andros Island, Bahamas, in Carew, J.L., (Ed.), *Proceedings*
847 *of the Eighth Symposium on the Geology of the Bahamas*, Bahamian Field
848 Station, San Salvador, Bahamas, 13-32, 1997.
- 849 Bobba, A.G.: Numerical modeling of salt-water intrusion due to human activities and
850 sea-level change in the Godavari Delta, India, *Hydrolog. Sci. J.*, 47, 67-80, 2002.

- 851 Bowleg, J. and Allen, D.M.: Effects of storm surges on groundwater resources, North
852 Andros Island, Bahamas. In: Treidgel H, Martin-Bordes JL and Gurdak JJ (Eds.).
853 Climate Change Effects on Groundwater Resources: A Global Synthesis of
854 Findings and Recommendations. IAH International Contributions to
855 Hydrogeology, CRC Press, London, UK, 2011.
- 856 Bukowski, J.M., Carney, C., Ritzi, R.W. Jr. and Boardman, M.R.: Modeling the fresh-salt
857 water interface in the Pleistocene aquifer on Andros Island, Bahamas, in Curran,
858 H.A., and J.E. Mylroie (Eds.), Proceedings of the Ninth Symposium on the
859 Geology of the Bahamas, Bahamian Field Station, San Salvador, Bahamas, 1-13,
860 1999.
- 861 Cant, R.V. and Weech, P.S.: A review of the factors affecting the development of
862 Ghyben-Herzberg lenses in the Bahamas, *J. Hydrol.*, 84, 333-343, doi:
863 10.1016/0022-1694(86)90131-9, 1986.
- 864 Cashman, A., Nurse, L. and Charlery, J.: Climate change in the Caribbean: the water
865 management implications, *The Journal of Environment and Development* 19(1),
866 42-67, doi: 10.1177/1070496509347088, 2010.
- 867 Chui, T. F. M., and Terry, J.P.: Modeling fresh water lens damage and recovery on atolls
868 after storm-wave washover. *Ground Water*, 50(3), 412-420, 2012.
- 869 Chui, T.F. and Terry, J.P.: Influence of sea-level rise on freshwater lenses of different
870 atoll island sizes and lens resilience to storm-induced salinization, *J. Hydrol.*, 502,
871 18-26, 2013.
- 872 Falkland, A. (Ed.): Hydrology and water resources of small island: a practical guide,
873 United Nations Educational, Scientific, and Cultural Organization (UNESCO),
874 Paris, 1991.
- 875 Franklin, J., Pasch, R., Avila, L., Beven, J., Lawrence, M., Stewart, S., and Blake, E.:
876 Atlantic hurricane season of 2004. *Monthly Weather Review*, 134(3): 981-1025,
877 2006.
- 878 Freeze, R.A., and Cherry, J.A.: *Groundwater*, Prentice-Hall, Upper Saddle River, NJ,
879 USA, 1977.
- 880 Goderniaux, P., Brouyere, S., Fowler, H.J., Blenkinsop, S., Therrien, R., Orban, P. and
881 Dassargues, A.: Large scale surface-subsurface hydrological model to assess
882 climate change impacts on groundwater reserves. *J. Hydrol.*, 373(1-2), 122-138,
883 2009.

- 884 Green, T. R., Taniguchi, M., Kooi, H., Gurdak, J.J., Allen, D.M., Hiscock, K.M. and
885 Aureli, A.: Beneath the surface of global change: Impacts of climate change on
886 groundwater, *J. Hydrol.*, 405 (3-4), 532-560, doi: 10.1016 /j.jhydrol.2011.05.002,
887 2011.
- 888 Guo, W. and Langevin, C.D.: User's guide to SEAWAT: A computer program for
889 simulation of three-dimensional variable-density ground-water flow, U.S.
890 Geological Survey Techniques and Methods Book 6, Chapter A7, Florida, USA,
891 2002.
- 892 Illangasekare, T., Tyler, S.W., Clement, T.P., Villholth, K.G., Perera, A.P.G.R.L.,
893 Obeysekera, J., Gunatilaka, A., Panabokke, C.R., Hyndman, D.W., Cunningham,
894 K.J., Kaluarachchi, J.J., Yeh, W.W.G., van Genuchten, M.T., and Jensen, K.:
895 Impacts of the 2004 tsunami on groundwater resources in Sri Lanka, *Water*
896 *Resour. Res.*, 42, W05201, doi: 10.1029/2006WR004876, 2006.
- 897 IPCC (2007), *Climate Change 2007: The Physical Science Basis*. S. Solomon, D. Qun,
898 M. Manning, Z. Chen, M. Marquis, K.B. Averyt, M. Tignor and H.L. Miller
899 (Eds.). Contribution of Working Group I to the Fourth Assessment Report of the
900 Intergovernmental Panel on Climate Change, Cambridge University Press,
901 Cambridge, UK.
- 902 IPCC (2014). *Climate Change 2014: Impacts, Adaptation, and Vulnerability. Part B:*
903 *Regional Aspects. Contribution of Working Group II to the Fifth Assessment*
904 *Report of the Intergovernmental Panel on Climate Change [Barros, V.R., C.B.*
905 *Field, D.J. Dokken, M.D. Mastrandrea, K.J. Mach, T.E. Bilir, M. Chatterjee, K.L.*
906 *Ebi, Y.O. Estrada, R.C. Genova, B. Girma, E.S. Kissel, A.N. Levy, S.*
907 *MacCracken, P.R. Mastrandrea, and L.L. White (eds.)]. Cambridge University*
908 *Press, Cambridge, United Kingdom and New York, NY, USA.*
- 909 Jyrkama, M.I., and Sykes, J.F.: The impact of climate change on spatially varying
910 groundwater recharge in the grand river watershed (Ontario), *J. Hydrol.*, 338, 237-
911 250, doi: 10.1016/j.jhydrol.2007.02.036, 2007.
- 912 Langevin C.D., Thorne, D.T., Dausman, A.M., Sukop, M.C. and Guo, W.: SEAWAT
913 Version 4: A Computer Program for Simulation of Multi-Species Solute and Heat
914 Transport: US Geol. Surv. Techniques and Methods Book 6, Chapter A22,
915 Florida, USA, 2007.
- 916 Langevin, C.D. and Zygnerski, M.: Effect of sea-level rise on salt water intrusion near
917 coastal well field in southeastern Florida, *Ground Water*, 51(5), 781-803, 2013.

- 918 Little, B.G., Buckley, D.K., Jefferiss, A., Stark, J. and Young, R.N.: Land resources of
919 the commonwealth of the Bahamas, Volume 4 Andros Island, Land Resources
920 Division, Tolworth Tower, Surrey, England, 1973.
- 921 McSweeney, C., New, M., Lizcano, G. and Lu, X.: The UNDP Climate Change Country
922 Profiles, B. Am. Meteorol. Soc., 91, 157-166, doi: 10.1175/2009BAMS2826.1,
923 2010.
- 924 Michael, H.A., Russoniello, C.J. and Byron, L.A.: Global assessment of vulnerability to
925 sea-level rise in topography-limited and recharge-limited coastal groundwater
926 systems, *Water Resour. Res.*, 49 (4), 2228-2240, doi:10.1002/wrcr.20213, 2013.
- 927 Mollema, P.N., and Antonellini, M.: Seasonal variation in natural recharge of coastal
928 aquifers, *Hydrogeol. J.*, 21, 787-797, doi: 10.1007/s10040-013-0960-9, 2013.
- 929 Momi, K., Shoji, J. and Nakagawa, K.: Observations and modeling of seawater intrusion
930 for a small limestone island aquifer, *Hydrol. Process.*, 19, 3897-3909, doi:
931 10.1002/hyp.5988, 2005.
- 932 NOAA (2014). <http://www.nhc.noaa.gov/> [accessed on June 10, 2014]
- 933 Obeysekera J., Park, J., Irizarry-Ortiz, M., Barnes, J. and Trimble, P.: Probabilistic
934 projection of mean sea level and coastal extremes, *Journal of Waterways and
935 Ports Coastal and Ocean Engineering*, 139 (2), 135-41, doi:
936 10.1061/(ASCE)WW.1943-5460.0000154, 2013.
- 937 Oude Essink, G.H.P.: Improving fresh groundwater supply – problems and solutions,
938 *Ocean and Coastal Management*, 44, 429-449, doi: 10.1016/S0964-
939 5691(01)00057-6, 2001.
- 940 Rahmstorf, S.: A semi-empirical approach to projecting future sea-level rise, *Science*,
941 315, 368-370, doi: 10.1126/science.1135456, 2007.
- 942 Ranjan, P., Kazama, S., Sawamoto, M. and Sana, A.: Global scale evaluation of coastal
943 fresh groundwater resources, *Ocean and Coastal Management*, 52, 197-206, doi:
944 10.1016/j.ocecoaman.2008.09.006, 2009.
- 945 Rasmussen, P., Sonnenborg, T.O., Goncear, G. and Hinsby, K.: Assessing impacts of
946 climate change, sea level rise, and drainage canals on saltwater intrusion to coastal
947 aquifer, *Hydrol. Earth Syst. Sci.*, 17, 421-443, doi: 10.5194/hess-17-421-2013,
948 2013.

- 949 Ritzi, R., Bukowski, J., Carney, C. and Boardman, M.: Explaining the thinness of the
950 fresh water lens in the Pleistocene carbonate aquifer on Andros Island,
951 Bahamas, *Ground Water*, 39 (5), 713-720, doi: 10.1111/j.1745-
952 6584.2001.tb02361.x, 2001.
- 953 Robins, N., and Lawrence, A.: Some hydrogeological problems peculiar to various types
954 of small islands, *Water Environ. J.*, 14 (5), 341-346, 2000.
- 955 Schneider, J., and Kruse, S.: A comparison of controls on freshwater lens morphology of
956 small carbonate and siliciclastic islands: Examples from barrier islands in Florida,
957 USA, *J. Hydrol.*, 284 (1-4), 253-269, doi: 10.1016/j.jhydrol.2003.08.002, 2003.
- 958 Schroeder, P.R., Dozier, T.S., Zappi, P.A., McEnroe, B.M., Sjostrom, J.W. and Peyton,
959 R.L.: The Hydrologic Evaluation of Landfill Performance (HELP) model:
960 Engineering documentation for Version 3, Rep. EPA/600/R-94/168b, U.S.
961 Environmental Protection Agency, Washington, D.C., USA, 1994.
- 962 Scibek, J., and Allen, D.M.: Modeled impacts of predicted climate change on recharge
963 and groundwater levels, *Water Resour. Res.*, 42 (11), W11405, doi:
964 10.1029/2005WR004742, 2006.
- 965 Stoeckl, L., and Houben, G.: Flow dynamics and age stratification of freshwater lenses:
966 Experiments and modeling, *J. Hydrol.*, 458, 9-15, doi:
967 10.1016/j.jyhrol.2012.05.070, 2012.
- 968 Sulzbacher, H., Wiederhold, H., Siemon, B., Grinat, M., Igel, J., Burschil, T., Günther, T.
969 and Hinsby, K.: Numerical modeling of climate change impacts on freshwater
970 lenses on the North Sea Island of Borkum using hydrological and geophysical
971 methods, *Hydrol. Earth Syst. Sci.*, 16 (10), 3621-3643, doi: 10.5194/hess-16-
972 3621-2012, 2012.
- 973 Tarbox, K.L.: Occurrence and development of water resources in The Bahamas, in H.A.
974 Curran (Ed.), *Proceedings of the Third Symposium on the Geology of the*
975 *Bahamas*, Bahamian Field Station, San Salvador, Bahamas, 139-144, 1987.
- 976 Terry, J.P., and Falkland, A.C.: Responses of atoll freshwater lenses to storm-surge
977 overwash in the Northern Cook Islands, *Hydrogeol. J.*, 18, 749-759, 2010.
- 978 Terry, J.P., and Chui, T.F.M.: Evaluating the fate of freshwater lenses on atoll islands
979 after eustatic sea-level rise and cyclone-driven inundation: A modeling approach,
980 *Global Planet Change*, 88-89, 76-84, doi: 10.1016/j.gloplacha.2012.03.008, 2012.

- 981 Therrien, R., McLaren, R., Sudicky, E. and Panday, S.: HydroGeoSphere – A three-
982 dimensional numerical model describing fully-integrated subsurface and surface
983 flow and solute transport, University of Waterloo and Université Laval,
984 Waterloo, Canada, 2010.
- 985 Toews, M.W., and Allen, D.M.: Evaluating different GCMs for predicting spatial
986 recharge in an irrigated arid region, *J. Hydrol.*, 374, 265-281, doi:
987 10.1016/j.jhydrol.2009.06.022, 2009
- 988 UNDP (United Nations Development Programme): Climate Change Country Profiles,
989 The Bahamas, 2010.
- 990 Vacher, H.L.: Dupuit-Ghyben-Herzberg analysis of strip-island lenses, *Bull. Geol. Soc.*
991 *Am.*,100,580-591,doi:10.1130/0016-606(1988)100<0580:DGHAOS>2.3.CO;2,
992 1988.
- 993 Vacher, H.L., and Quinn, T.M. (Eds.): Geology and hydrogeology of carbonate island,
994 *Developments in Sedimentology Vol. 54*, Elsevier, Tampa Bay, Florida, USA,
995 1997.
- 996 Wallis, T.N., Vacher, H.L. and Stewart, M.T.: Hydrogeology of freshwater lens beneath a
997 Holocene strandplain, Great Exuma, Bahamas, *J. Hydrol.*, 125, 93-109, doi:
998 10.1016/0022-1694(91)90085-V, 1991.
- 999 Werner, A.D., and Simmons, C.T.: Impact of sea-level rise on sea water intrusion in
1000 coastal aquifers, *Ground Water*, 47, 197-204, doi: 10.1111/j.1745-
1001 6584.2008.00535.x, 2009.
- 1002 Werner, A.D., Jakovovic, D. and Simmons, C.T.: Experimental observations of saltwater
1003 up-coning, *J. Hydrol.*, 373, 230-241, doi: 10.1016/j.jhydrol.2009.05.004, 2009.
- 1004 Whitaker, F., and Smart, P.: Climatic control of hydraulic conductivity of Bahamian
1005 limestones. *Ground Water*, 35(5), 859-868, doi: 10.1111/j.1745-
1006 6584.1997.tb00154.x, 1997.
- 1007 White, N.J., Church, J.A. and Gregory, J.M.: Coastal and global averaged sea level rise
1008 for 1950 to 2000, *Geophy. Res. Lett.*, 32, L01601, doi: 10.1029/2004GL021391,
1009 2005.
- 1010 White, I., and Falkland, A.: Management of freshwater lenses on small Pacific islands,
1011 *Hydrogeol. J.*, 18, 227-246, doi: 10.1007/s10040-009-0525-0, 2010.

- 1012 Wolfe, P.J., Adams, A.L. and Carney, C.K.: A resistivity study of the freshwater lens
1013 profile across North Andros Island, The Bahamas, in Greenstein, B.J., and C.K.
1014 Carney (Eds.), Proceedings of the Tenth Symposium on the Geology of the
1015 Bahamas and Other Carbonate Regions, Gerace Research Center, San Salvador,
1016 Bahamas, 31-40, 2001.
- 1017 WHO (World Health Organisation): Guidelines for drinking-water quality, 4th Edition,
1018 Geneva, Switzerland, 2011.
- 1019 Yang, J., Graf, T., Herold, M. and Ptak, T.: Modeling the effects of tides and storm
1020 surges on coastal aquifers using a coupled surface-subsurface approach, Journal of
1021 Contaminant Hydrology, 149, 61-75, 2013.
- 1022 [Younger, P.L.: Simple generalized methods for estimating aquifer storage parameters,](#)
1023 [Quarterly Journal of Engineering Geology and Hydrogeology, 26, 127-135, 1993.](#)
1024 [doi: 10.1144/GSL.QJEG.1993.026.02.04.](#)

1025 **Table 1. SEAWAT model parameters**

Parameter	Value
Model Domain	200 m deep; lateral extent based on island area
Lucayan/ Pre-Lucayan interface	40 mbgs
Paleosol Depths	9-10 mbgs and 14-15 mbgs
Hydraulic Conductivity	Lucayan: 864 m/day – paleosols: 8,640 m/day – Pre-Lucayan: 86,400 m/day
Specific Storage/ <u>Specific Yield</u>	$1 \times 10^{-5} \text{ m}^{-1}$ / <u>0.15</u>
<u>Effective Porosity</u>	<u>0.15</u>
Dispersivity	Longitudinal 1.0 m; Transverse (Vertical & Horizontal) 0.1 m
Specified Head Boundary	0 masl along model domain periphery; specified density 1.025 kg/L
Concentration at Specified Head Boundary	35 g/L along model domain periphery
Initial Concentration	35 g/L throughout model domain
Recharge	877 mm/year (north) and 426 mm/year (south); concentration 0 g/L
Time Steps	Initial: 14 minutes; Maximum: 1 day;

1026 **Table 2. Projected climate shifts for the 2090s, and the resulting projected**
 1027 **values for monthly mean temperature and monthly mean**
 1028 **precipitation for North and South Andros.**

Parameter	D	J	F	M	A	M	J	J	A	S	O	N
Temperature Shift (°C)	+2.8			+3.0			+3.2			+3.2		
Projected Monthly Mean Temperature (°C) <i>North/South</i>	25.2	24.3	24.6	25.3	26.8	28.5	30.4	31.3	31.3	30.9	32.7	27.7
Precipitation Shift (mm)	-2			-18			-24			+12		
Projected Monthly Mean Precipitation (mm) <i>North</i>	45	48	50	47	66	90	189	138	210	190	176	98
Projected Monthly Mean Precipitation (mm) <i>South</i>	51	34	37	24	27	89	81	40	57	112	138	103

1029

1030 **Table 3. Observed conditions used for calibrating the HGS model-criteria**

Parameter	Value
Recharge	877 mm/year
Vadose Zone Thickness	1.5-2 m
Water Table Elevation	2 masl
Hydraulic Conductivity	86—8,640 m/day
Gradient	0.0005 – 0.001
Porosity	0.15
Average Velocity	0.3 m/day
Thickness of Lens	15-20 m
Paleosols	9 and 14 mbgs

1031 **Table 4. HGS model parameters**

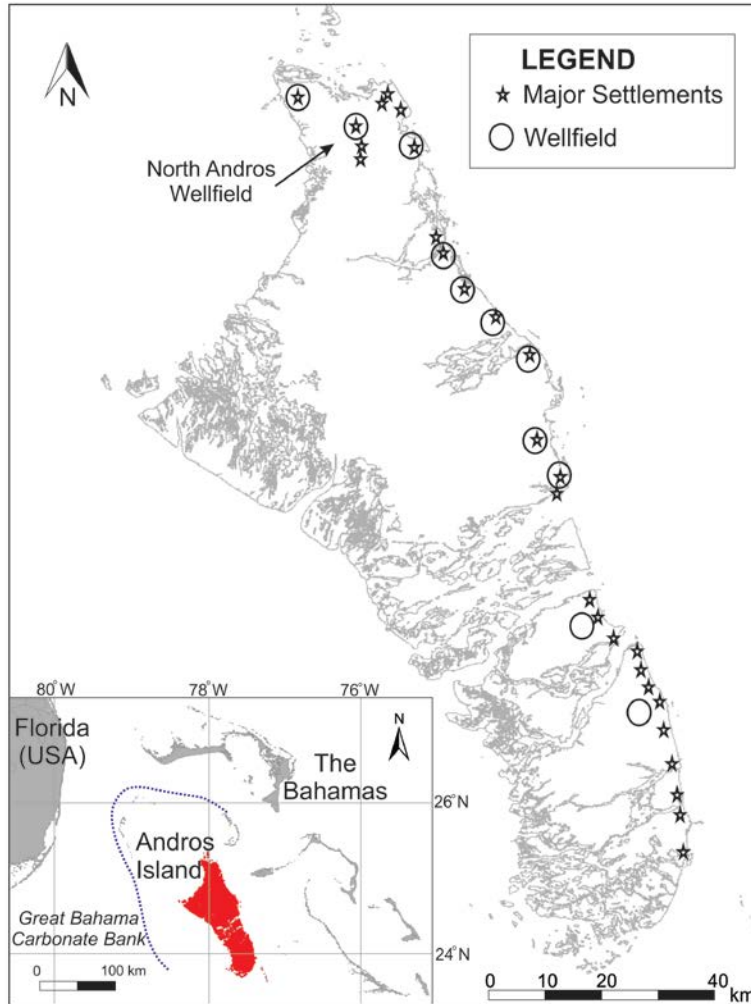
Parameter	Value
Model Domain	2,400 m model domain width; 43.5 m domain depth (representing Lucayan Limestone)
Paleosol Depths	9-10 mbgs and 14-15 mbgs
Trench Dimensions	1 m wide, 2 m deep.
Hydraulic Conductivity	Lucayan limestone: 86.4 m/day; paleosols: 864 m/day
Effective Porosity	0.15
Specific Storage	$1 \times 10^{-5} \text{ m}^{-1}$
Dispersivity	Longitudinal 1.0 m; Transverse Horizontal 0.1 m; Transverse Vertical 0.01 m
Specified Head Boundary	0 masl along model domain periphery; specified density 1.025 kg/L
Concentration at Specified Head Boundary	35 g/L along model domain periphery
Initial Concentration	35 g/L throughout model domain
Recharge	877 mm/year; concentration 0 g/L
Time Steps	Initial time step: 0.8 seconds Maximum time step: 1 day

1032

1033 **Table 5. Percent change in freshwater lens morphology relative to the baseline**
1034 **model for the combined effect of reduced recharge and sea level rise.**

Modeled Region	% Change Area	% Change Volume
Northern	-4.1	-5.9
Southern	-16.8	-24.2

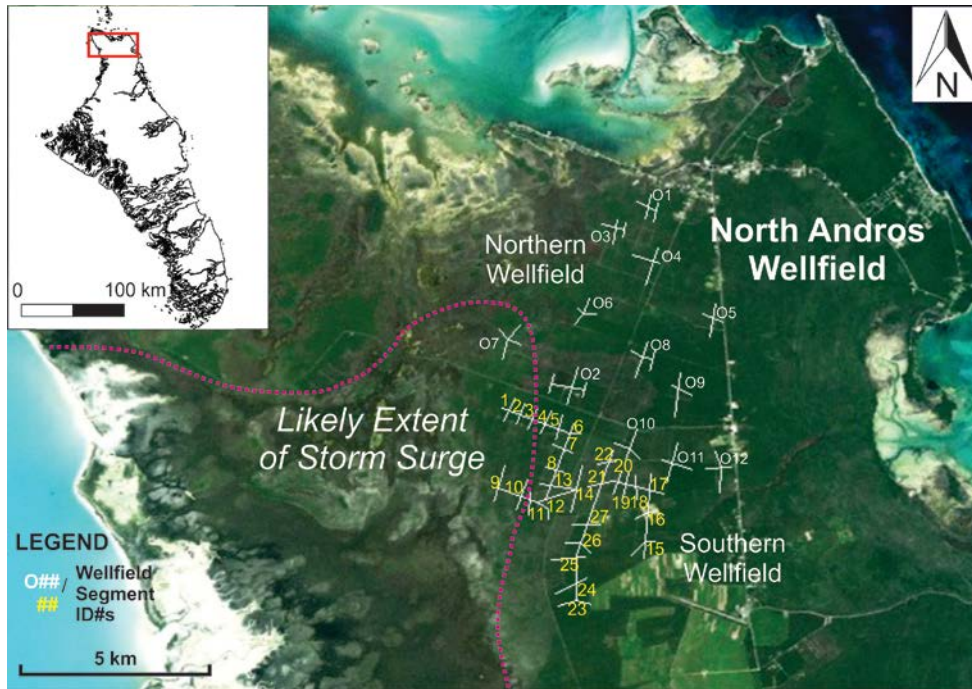
1035



1036

1037

Figure 1. Andros Island, indicating the location of settlements and wellfields.

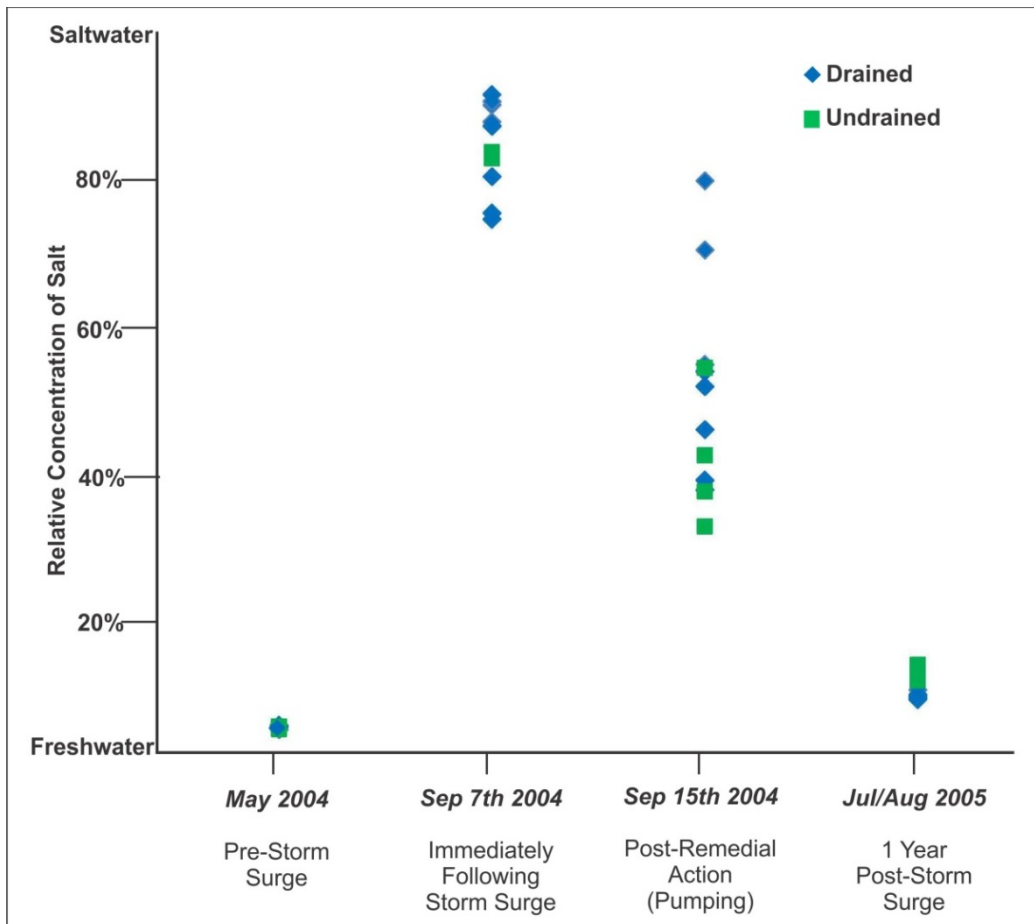


1038

1039

1040

Figure 2. Layout of the North Andros Wellfield indicating the likely extent of the 2004 Hurricane Frances storm surge overwash.



1041

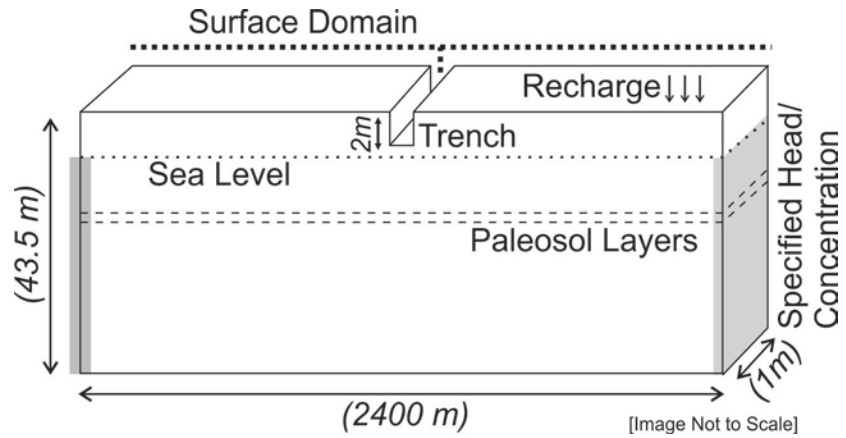
1042

1043

1044

Figure 3. Salinity monitoring data before and after the 2004 Hurricane Frances storm surge. Data are shown for the southern trench segments of the North Andros Wellfield only. See Figure 2 for the location of the trench segments.

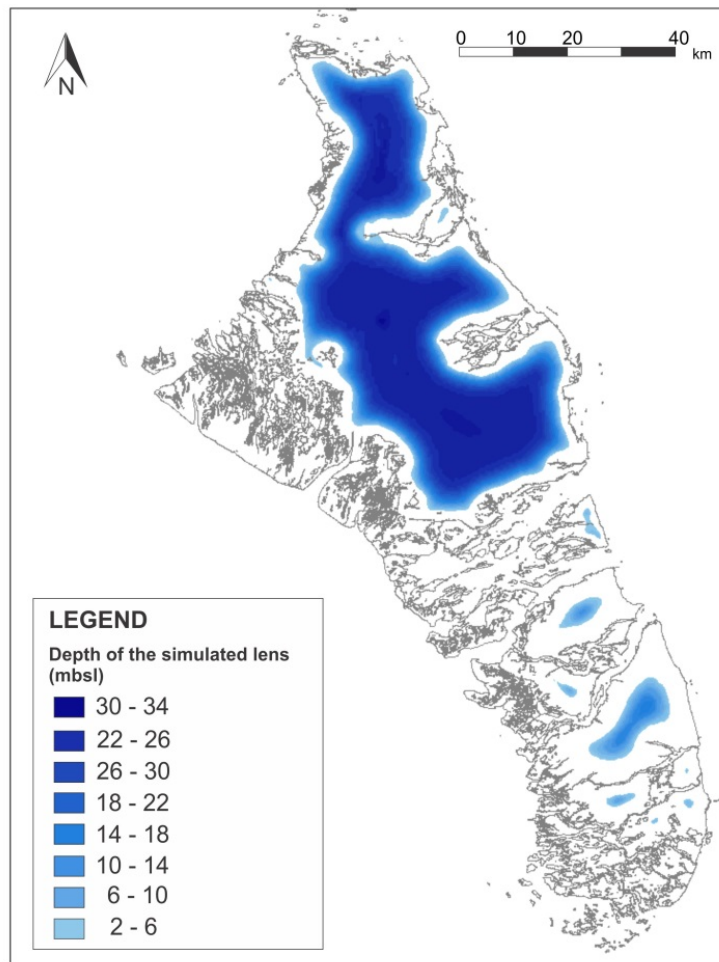
1045



1046

1047

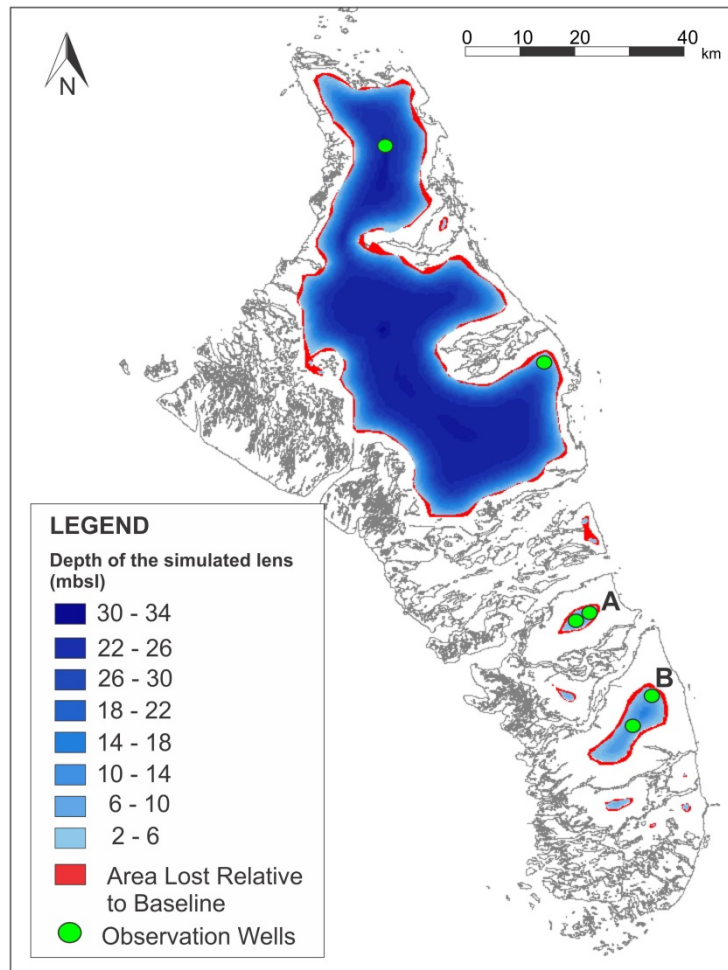
Figure 4. HydroGeoSphere model domain and boundary conditions.



1048

1049

Figure 5. Baseline freshwater lens representing current conditions.



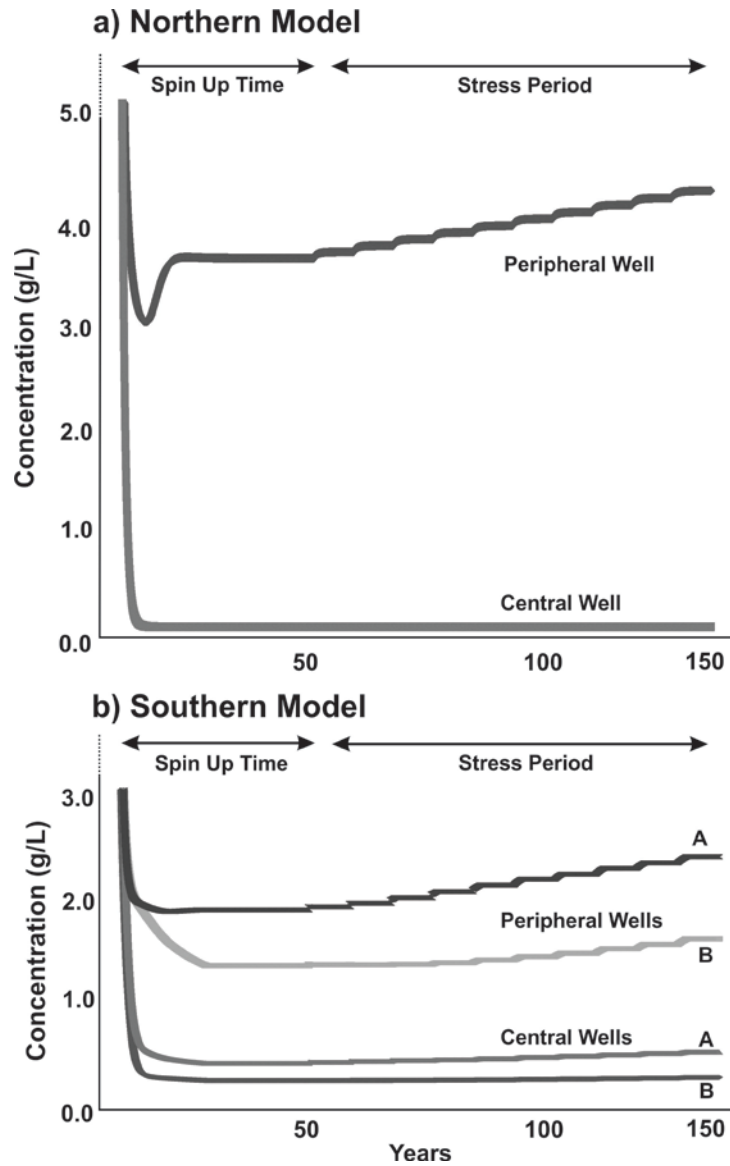
1050

1051

Figure 6. Model result for climate change simulations for the combined effect of reduced recharge and sea level rise, indicating area lost relative to baseline conditions.

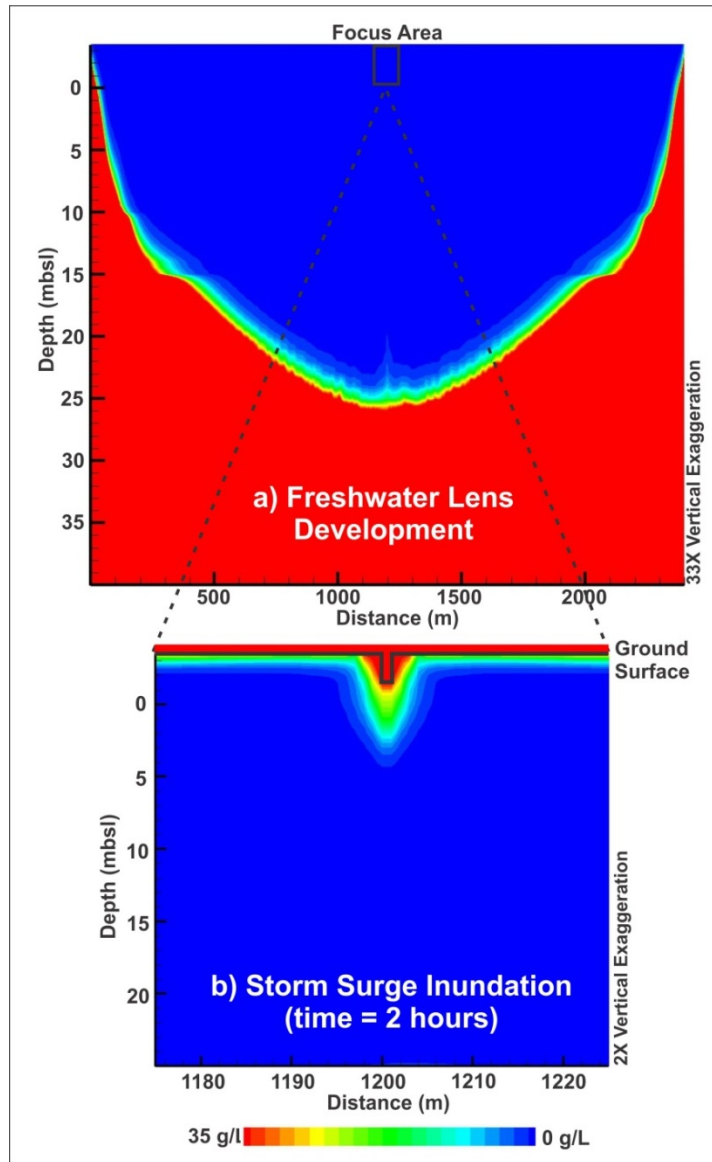
1052

1053



1054
 1055
 1056
 1057

Figure 7. Simulated dissolved salt concentrations over time at the observation wells for climate change models. a) northern model b) southern model with two observation wells for each landmass shown.

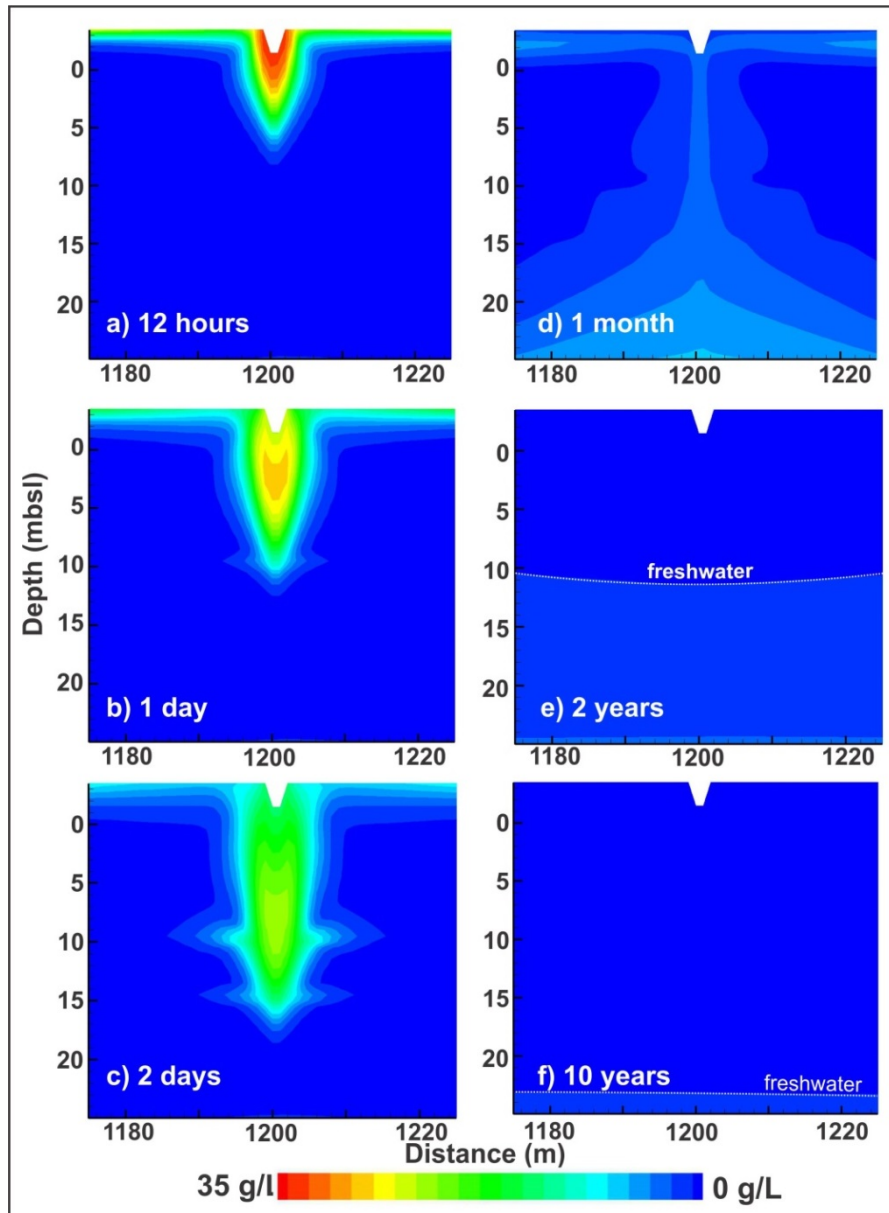


1058

1059

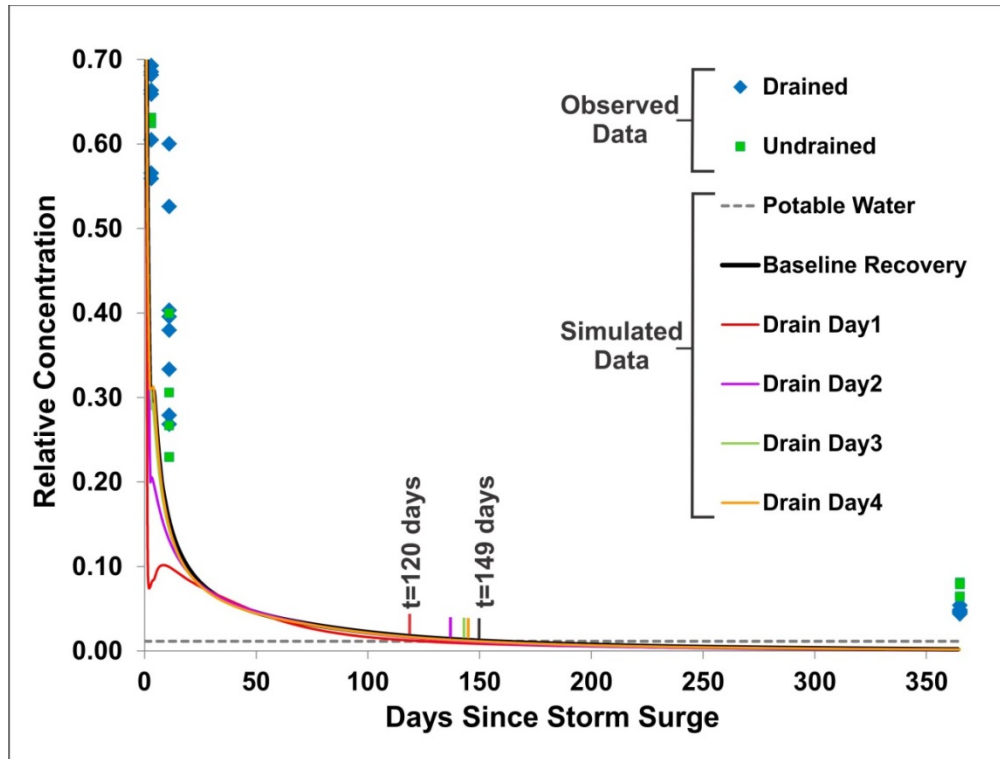
1060

Figure 8. a) Freshwater lens development after 50 years (Phase 1); b) Storm surge inundation in the focus area at 2 hours (Phase 2).



1061
 1062
 1063

Figure 9. Baseline recovery of the freshwater lens post storm surge at a) 12 hours; b) 1 day; c) 2 days; d) 1 month; e) 2 years and; f) 10 years.



1064

1065

Figure 10. Observed and simulated concentrations within the trench. The times for concentrations to reach potable water threshold are indicated by the small vertical bars for the baseline recovery scenario (149 days) and the various scenarios of draining on different days following the surge (120 days for draining on day 1). The increase in concentration observed for Scenario Drain Day 1 represents the end of the draining period, when high concentration water re-enters the trench from the surrounding aquifer and vadose zone.

1066

1067

1068

1069

1070

1071

1072